Mechanical properties of crosslinks controls failure mechanism of hierarchical intermediate filament networks

Zhao Qin,[1] and Markus J. Buehler[1,2,3,a)]

[1)] *Laboratory for Atomistic and Molecular Mechanics (LAMM), Department of Civil and Environmental Engineering, Massachusetts Institute of Technology, 77 Massachusetts Ave., Room 1-235 A&B, Cambridge, MA 02139, USA*

[2)] *Center for Computational Engineering, Massachusetts Institute of Technology, 77 Massachusetts Ave., Cambridge, MA 02139, USA*

[3)] *Center for Materials Science and Engineering, Massachusetts Institute of Technology, 77 Massachusetts Ave., Cambridge, MA 02139, USA*

(Received 13 October 2011; accepted 16 November 2011; published online 10 January 2012)

Abstract Intermediate filaments are one of the key components of the cytoskeleton in eukaryotic cells, and their mechanical properties are found to be equally important for physiological function and disease. While the mechanical properties of single full length filaments have been studied, how the mechanical properties of crosslinks affect the mechanical property of the intermediate filament network is not well understood. This paper applies a mesoscopic model of the intermediate network with varied crosslink strengths to investigate its failure mechanism under the extreme mechanical loading. It finds that relatively weaker crosslinks lead to a more flaw tolerant intermediate filament network that is also 23% stronger than the one with strong crosslinks. These findings suggest that the mechanical properties of interfacial components are critical for bioinspired designs which provide intriguing mechanical properties. [doi:10.1063/2.1201405]

Keywords failure mechanism, flow tolerance, intermediate filament, protein network, soft material, rupture, crosslink strength, bioinspired design

In eukaryotic cells, the network of actin microfilaments and microtubules in the cytoskeleton is accompanied by a third major filament system called intermediate filaments.[1–3] These fibrous proteins have been found in nearly all eukaryotic cells and many biological materials including wool, hair and hooves but are absent in both plants and fungi. Intermediate filaments arise from cell-type-specific expression of a complex gene family that in man encodes more than 70 proteins.[1,2] Its subunit has a common tri-partite organization characterized by a central alpha-helical coiled-coil domain and amorphous "head" and "tail" domains of variable length and sequence.[1] As other fibrous proteins such as collagen or fibrin, they linearly and laterally self assemble into filaments with a diameter of 8–12 nm.[3]

Intermediate filament networks in eukaryotic cells have developed to perform multiple functions, including stabilizing cells' conformation, integrating cells into tissues and organs, protecting genetic material and mediating mechanotransduction processes.[4–6] Vimentin is a specific type of intermediate filaments found in the cytoplasm of fibroblasts, leukocytes, and blood vessel endothelial cells, representing the most widely distributed type of intermediate filaments.[7] It is well accepted that vimentin plays a significant role in maintaining cell integrity by supporting and anchoring the position of the organelles in the cytoplasm.[7,8] Lamin, another type of intermediate filaments found at the inner membrane of the nuclear envelope of eukaryotic cells, contributes largely to the structural integrity of the cell nucleus and plays a vital biological role to protect genetic material against extreme conditions.[9,10] Therefore, intermediate filaments have been referred to as the "safety belts of cells". Besides their functions as mechanical integrators, over the last decade, intermediate filaments have also emerged as a key element in understanding signaling. For example, vimentin has been found to bind to isoforms of one of the major families of signaling proteins named 14-3-3.[5] It attenuates the response to specific proapoptotic signals in several cell cultures but promotes apoptosis once there is commitment to execute.

While it is known that single intermediate filaments are composed of bundles of subunits with hierarchical structures, from coiled-coil dimer level to the full length filament level as shown in Fig. 1(a),[1] it is not clear how full length filaments associate to form a network structure, and in particular how the change of the chemical nature of their association can affect the particular mechanical and physiological function of the network. For example, divalent cations, such as Ca^{+} and Mg^{+}, have been recognized as widely observed crosslinking agents in the vimentin network and their concentration can affect the stiffness of the entire filament network.[11] Plectin, a protein with coiled-coil structure, plays a role as linker to connect cytoskeletal filaments and is important for network organization and mechanical properties.[12] In this paper, we do not restrict the focus on the role of any specific crosslinking agent but, for a more general purpose, we model both the intermediate filament and the crosslinks with varied mechanical properties and study how the strength

a)Corresponding author. Email: mbuehler@MIT.EDU.

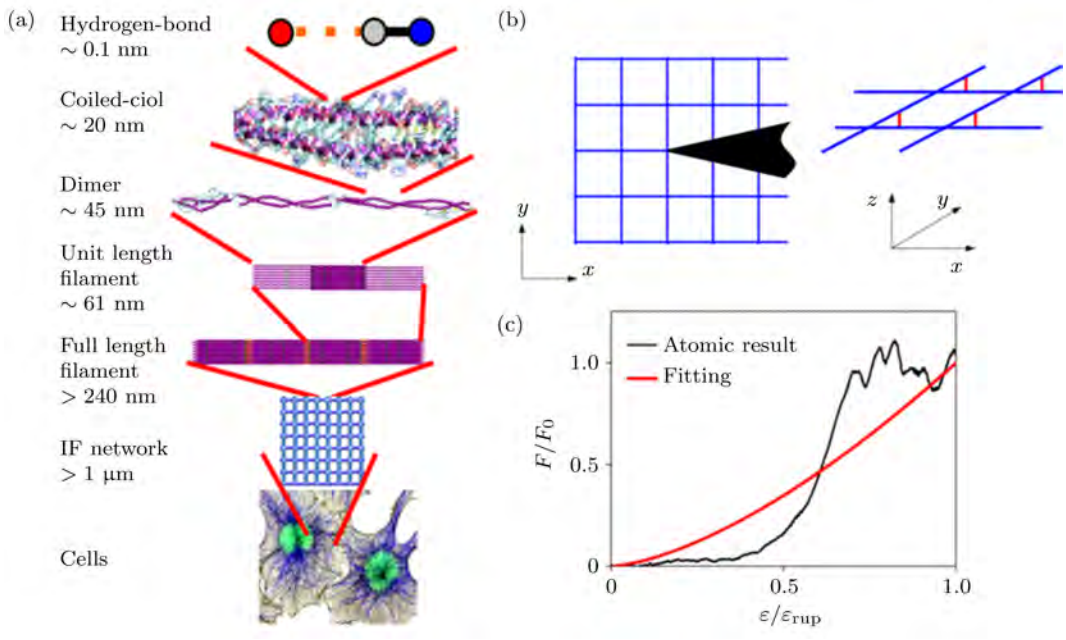

Fig. 1. Structural and mechanical properties of intermediate filaments and intermediate filament networks. (a) The hierarchical structures of intermediate filament, from atomic level to network level. (b) The configuration of the network structure near the crack tip used in this study: blue for the intermediate filament, red for the crosslink and black shadowed part for the one end of the initial crack. (c) The force-strain relationship of a full length filament. This plot contains both the result of atomic simulation[8] and the corresponding fitting curve given by Eq. (2) with a result of $\varepsilon_{\text{rup}} = 2.6$ and $N = 1.5$.

of the crosslink affects the mechanical behavior of the overall intermediate filament network.

The structure of the network used in this study is composed of intermediate filaments distributed independently in the x- and y-directions and they are pinned by crosslinks at their intersections shown in Fig. 1(b). This set up broadly mimics the microscopic structure of the Xenopus oocyte nuclear lamina.[13–15] Realistic structures of intermediate filament network can be more disordered and/or have slightly variegated structures, but our model represents an approximation to the network. We focus on how the mechanical property of the crosslink affects the failure of intermediate filament network, while other factors such as chemical reactions are not included in our work. This is motivated by the fact that maintaining the mechanical integrity of cell is one of the most important functions of intermediate filament networks.[16–18]

We use a mesoscopic model to describe each intermediate filament as a series of beads interacting according to nonlinear interparticle multibody potentials. The total energy is given by

$$E_x = \sum_{\text{pair}} \varphi_T(\varepsilon) + \sum_{\text{triplets}} \varphi_{\text{B}}(\theta). \tag{1}$$

For general purpose, the force tensile strain curve $F_T(\varepsilon)$ of each single intermediate filament is modeled by a power-law function as

$$F_T(\varepsilon) = -\partial\varphi_T(\varepsilon)/(r_0\partial\varepsilon) = F_0(\varepsilon/\varepsilon_{\text{rup}})^N f(\varepsilon), \tag{2}$$

where F_0 is the strength of a full length filament, ε_{rup} is the corresponding strain for F_0, N is the so-called hardening exponent which describes the nonlinear stress-strain response of a material. For a crosslink, the force response under deformation is given by a similar expression as Eq. (1) except for that the strength is given by another independent term $F_{\text{c\_0}}$. For the hardening exponent, $N < 1$ denotes softening behavior (also referred to as "elastic-plastic") of the material, $N = 1$ denotes linear behavior and $N > 1$ represents a stiffening material.[13] The expression $f(\varepsilon)$ is a cut-off function as $f = 1$ for $\varepsilon < \varepsilon_{\text{rup}}$ and $f = 0$ for $\varepsilon \geq \varepsilon_{\text{rup}}$; and typical force tensile strain curves of a full length filament is given in Fig. 1(c).[8] For simplicity, the force expression included in this study is normalized by the strength of the full length filament. The bending energy of each filament is given by

$$\varphi_{\text{B}}(\theta) = \frac{1}{2}k_{\text{B}}(\theta - \theta_0)^2, \tag{3}$$

with k_{B} relating to the bending stiffness of the intermediate filament EI through $k_{\text{B}} = 3EI/r_0$, EI relates to the intermediate filament persistence length L_p through $EI = L_p K_{\text{B}} T$, where K_{B} is the Boltzmann constant and T is the temperature. All the parameters of the modeling are summarized in Table 1.

The meshwork model shown in Fig. 1(b) includes 24 filaments in the y-direction (1.2 μm) and 24 filaments (1.2 μm) in the x-direction, with a crack-like defect added in the center to mimic a structural imperfection. Filaments at the orthogonal corners are mechanically

Table 1. Geometric and numerical parameters for the computational model.

Parameter and units	Numerical value
Equilibrium bead distance r_0/nm	5
Equilibrium distance of crosslink r_{c_0}/nm	2
Filament diameter D/nm	10
Lattice constant d/nm	50
Strength of each filament F_0/nN	7.9
Overall hardening exponent N	1.5
Bond breaking strain $\varepsilon_{\mathrm{rup}}$	2.6
Equilibrium angle θ_0/rad	π
Bending stiffness parameter k_{B}/(kcal $\cdot$ mol^{-1} $\cdot$ rad^{-2})	169.51
Mass of each mesoscale particle/amu	230 913
Density ρ/kg $\cdot$ m^{-3}	260

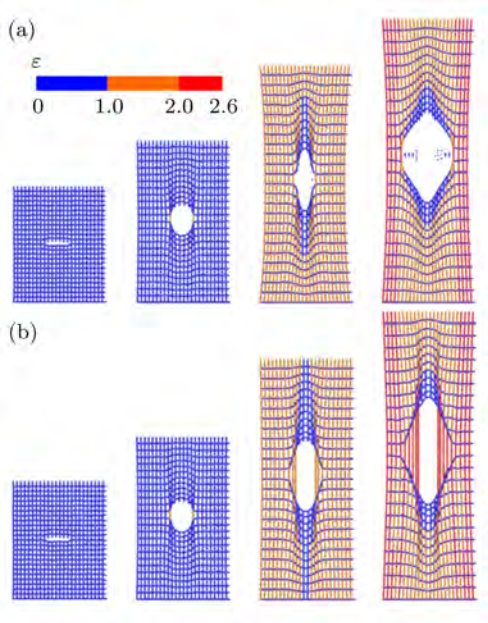

Fig. 2. Simulation snapshots of the conformations of intermediate filament networks under different applied strains (from left to right) of 0.22, 0.70, 1.50 and 2.00. (a) Intermediate filament network with crosslink strength of $F_{c\_0} = F_0$. (b) Intermediate filament network with crosslink strength of $F_{c\_0} = 0.2F_0$. Each of the filaments is colored according to its local tensile strain given by the color bardepicted in panel (a).

cross-linked by chemical interaction in our model. All simulations reported here are carried out in two steps by LAMMPS package.[19] First, we perform a relaxation during which we equilibrate the system. Relaxation is achieved by energy minimization, the system is heated up from 0 K to 300 K, then the structure is annealed at a temperature of 300 K. Second, we perform a loading simulation during which we keep the system at 300 K and apply a constant strain rate of 8.0×10^{-3} ns^{-1} to continuously increase the loading applied to the bottom and top layers of beads.

To examine the effect of the crosslink strength on the failure mechanism of intermediate filament network, we apply tensile force to the intermediate filament network with different crosslink strengths, F_{c_0}. The conformational changes of the networks under tension with two typical crosslink strengths are summarized in Fig. 2. The network models of $F_{c\_0} = F_0$ and $F_{c\_0} = 0.2F_0$ show rather different deformation and failure mechanisms under tension visualized in Figs. 2(a) and 2(b), respectively. It is observed that for the case with strong cross-links ($F_{c\_0} = F_0$), the network fails by breaking filaments at the crack tip with the increasing tensile force and the crack propagates in the initial direction of the initial crack orientation. For the network with weaker cross-links ($F_{c\_0} = 0.2F_0$) the crack does not propagate. Rather, the tensile force unpins the filaments in the x-direction from the filaments in the y-direction by breaking the crosslinks. This failure mechanism facilitates a "diffusion" of the deformation energy at the crack tip and renders the deformation within the filaments more uniform in the y-direction. This can be directly confirmed in the visual representations. Moreover, this unpinning step affects the flaw tolerance of the network material by increasing its tensile strength as shown in Fig. 3(a). The overall strength F_{net} of the entire network increases from $15.0F_0$ to $18.4F_0$, and the failure strain increases from 2.2 to 2.5 as the strength of the crosslinks decreases from F_0 to $0.2F_0$.

We now study the maximum stress of the network by using $\sigma_F = F_{\mathrm{net}}/(24dD)$, where d is the lattice constant of the network and D is the diameter of the filament. Its relationship with the strength of the crosslinks is shown in Fig. 3(b). Instead of a gradual transition, the decreasing strength of the crosslink increases the maximum stress of the network exponentially, and by 23% between $F_{c\_0} = 0.5F_0$ and $0.2F_0$. This leads to the most important result of this paper: a relatively weaker crosslink increases the strength of the overall intermediate filament network. This result is counterintuitive but makes sense because the rupture of crosslinks before reaching the strength limit of the filaments at the crack tip efficiently decreases the force concentration at the crack tip. Thereby, it efficiently increases the maximum applied loading before failure occurs.

To find an analytical solution of the particular crosslink strength which leads to an increased robustness of the intermediate filament network, we assess the geometric details and force distribution around the crack tip. Based on the fact that the initial crack deforms to an elliptical shape before failure we have $\mathrm{d}x/\mathrm{d}y\big|_{x=a} = 0$ at the crack tip along the inner crack surface, a denotes the half length of the crack in the x-direction. Therefore, including the fact that intermediate filaments are flexible in bending, we achieve the balance of force in tension via $F_1 = F_2 + F_3$, where F_1 is the tension force within the filament at the crack tip, F_2 is the tension force exerted from the neighboring lattice in the tensile direction, and F_3 is the tension force exerted from the crosslink illustrated in Fig. 3(b).The rupture

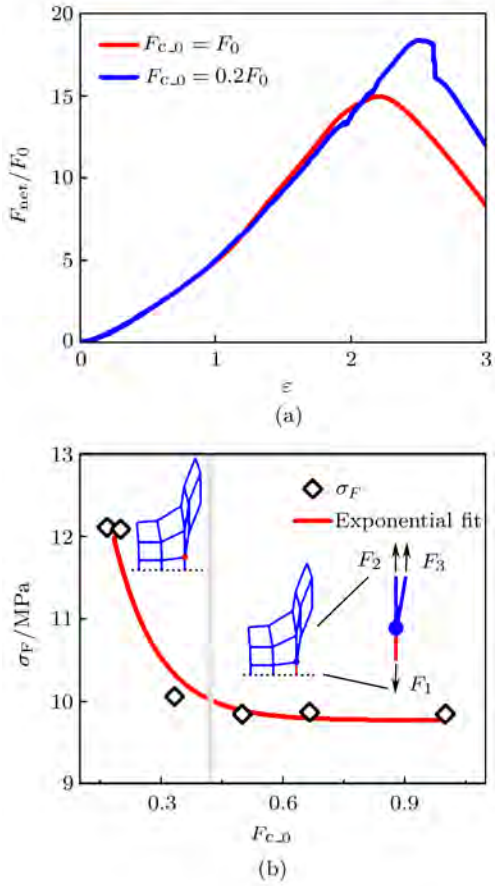

Fig. 3. Mechanical response of intermediate filament network under tension. (a) Overallforce-extension curve of the network with strong crosslinks ($F_{c\_0} = F_0$) and weak crosslinks ($F_{c\_0} = 0.2F_0$). (b) The tensile strength of the network with different crosslink strengths. The weak crosslink increases the tensile strength of the network by switching the failure mechanism from failure of filaments at the crack tip (right to the bar) to failure of the crosslinks (left to the bar). The gray bar corresponds to the critical condition that $F_{c\_0} = 0.42F_0$ as obtained.

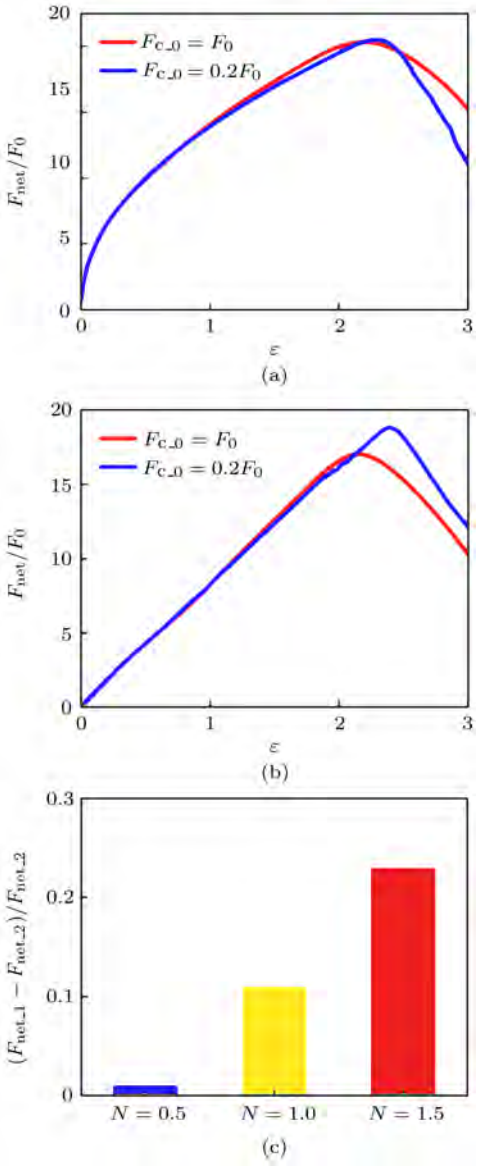

Fig. 4. Force-extension curve of networks with different mechanical characteristics under tension. (a) By using $N = 0.5$ in Eq. (2) to give the characteristic of strain-softening materials. (b) By using $N = 1$ in Eq. (2) to give the characteristic of linear elastic materials. Each of those networks is tested with two typical crosslinks strengths F_0 and $0.2F_0$. (c) Increment of the strength of the network (F_{net_1}) with weak crosslinks ($F_{c\_0} = 0.2F_0$) comparing to that (F_{net_2}) of the network with strong crosslinks ($F_{c\_0} = F_0$). Results of three typical materials with different N are summarized here for comparison.

condition of the filament at the crack tip is $F_1 = F_0$, which corresponds to the rupture strain ε_{rup}. Under the condition that there is no rupture event of crosslinks, the applied tensile force to the network near the crack tip is proportional to $1/\sqrt{r}$,[20] where r is the distance from the middle of the filament to the crack tip. We have $F_2 = F_1(\sqrt{r_1/r_2})$, where r_1 is the distance from the middle of the filament with F_1 in tension to the crack tip and r_2 is the distance from the middle of the filament with F_2 in tension to the crack tip. Therefore, the condition

$$F_3 < F_0(1 - \sqrt{r_1/r_2}) \tag{4}$$

is the necessary condition to prevent rupture of the filament at the crack tip before rupture of the crosslink occurs. As we have $r_1 = 0.5d$ and $r_2 = 1.5d$ for the geometry of this lattice model, $F_3 < 0.42F_0$ as the necessary condition is obtained (as shown in Fig. 3(b)). Indeed, it is shown by our simulations that networks with crosslinks weaker than this critical value are stronger under tension. It is also noted that this condition does not directly correspond to the maximum strength because of the nonlinearity of the stress distribution around the crack tip of such a strain-hardening material.

To investigate if this unpinning process exists for

materials with mechanical responses which are significantly different from what intermediate filament display, we test other two materials with typical force-extension curves of $N = 0.5$ and $N = 1.0$ as given by Eq. (2). Each of them represents a strain-softening and linear elastic material, respectively. For each of the materials, we obtain the stress-extension curves for crosslink strengths of $F_{c\_0} = F_0$ and $0.2F_0$ as shown in Figs. 4(a) and 4(b), respectively. We find that the increments of the network strength caused by the weak crosslink of those two materials are only 1% and 11%, which are significantly smaller than that of the strain-hardening material as for intermediate filament network (23%) summarized in Fig. 4(c).

In summary, here we identified two different failure mechanisms of intermediate filament networks under tension. We found that the strength of the crosslink between the filaments plays a critical role in defining the failure mechanism of the network, where the unpinning process between crosslinked flaments is the key mechanism to enable this behavior. Comparing to the failure of the network with strong crosslinks, we find that the networks with relatively weak crosslinks are 23% stronger than the former. We compared this result to other materials with different nonlinear mechanical responses and found that this switching function controlled by crosslink strength is only significant for strain-hardening materials. This mechanical characteristic, a significant stiffening of the material behavior with larger deformation, is indeed shared by many biological materials including intermediate filaments, spider silk, amyloids and collagen, and many others.[21,22]

This work was supported by AFOSR and ONR-PECASE.

1. H. Herrmann, H. Bar, and L. Kreplak, et al., Nature Reviews Molecular Cell Biology **8**, 562 (2007).
2. M. B. Omary, P. A. Coulombe, and W. H. I. McLean, New England Journal of Medicine **351**, 2087 (2004).
3. H. Ishikawa, R. Bischoff, and H. Holtzer, Journal of Cell Biology **38**, 538 (1968).
4. N. Wang, and D. Stamenovic, American Journal of Physiology-Cell Physiology **279**, C188 (2000).
5. P. A. Coulombe, and S. Kim, Genes & Development **21**, 1581 (2007).
6. N. Wang, and Z. G. Suo, Biochemical and Biophysical Research Communications **328**, 1133 (2005).
7. H. Herrmann, M. Haner, and M. Brettel, et al., Journal of Molecular Biology **264**, 933 (1996).
8. Z. Qin, L. Kreplak, and M. J. Buehler, PLoS One **4**, e7294 (2009).
9. K. N. Dahl, S. M. Kahn, and K. L. Wilson, et al., J. Cell Sci. **117**, 4779 (2004).
10. K. N. Dahl, P. Scaffidi, and M. F. Islam, et al., Proceedings of the National Academy of Sciences of the United States of America **103**, 10271 (2006).
11. D. A. Weitz, Y. C. Lin, and C. P. Broedersz, et al., Journal of Molecular Biology **399**, 637 (2010).
12. G. Wiche, Journal of Cell Science **111**, 2477 (1998).
13. Z. Qin, and M. J. Buehler, Acs Nano **5**, 3034 (2011).
14. M. W. Goldberg, J. Fiserova, and I. Huttenlauch et al., Biochemical Society Transactions **36**, 1339 (2008).
15. U. Aebi, J. Cohn, and L. Buhle, et al., Nature **323**, 560 (1986).
16. P. Panorchan, B. W. Schafer, and D. Wirtz, et al., J. Biol. Chem. **279**, 43462 (2004).
17. M. J. Buehler, and Y. C. Yung, Nature Materials **8**, 175 (2009).
18. J. Bertaud, Z. Qin, and M. J. Buehler, Acta Biomaterialia **6**, 2457 (2010).
19. S. Plimpton, Journal of Computational Physics **117**, 1 (1995).
20. L. B. Freund, *Dynamic Fracture Mechanics* (CUP, Cambridge, 1990).
21. S. Keten, Z. P. Xu, and B. Ihle, et al., Nature Materials **9**, 359 (2010).
22. Z. P. Xu, R. Paparcone, and M. J. Buehler, Biophysical Journal **98**, 2053 (2010).